

## Supplementary Information

### **Freestanding organogels by molecular velcro of unsaturated amphiphiles**

Vijai Shankar Balachandran, Kizhmuri P. Divya, Malick Samateh, Sai S. Sagiri, Sitakanta Satapathy, Padmanava Pradhan, Srinivasa R. Raghavan, Leela Rakesh,\* Michael S. Sellers, Shashi P. Karna,\* and George John\*

## **Table of Contents**

## **Page number**

1. Experimental Section	P3
2. Computational Details	P4-P5
3. Rheology	P5-P6
4. $^2\text{H}$ NMR studies	P6-P7
5. Gelation studies	P7
6. Molecular simulations	P8
7. Textural profile analysis	P9
8. DPD Simulation	P9-P13
9. References	P13

## 1. Experimental Section

**Chemicals and Reagents:** Cardanol was obtained by double vacuum distillation of cashew nut shell liquid at  $(3 \pm 4)$  mm Hg in which the fraction boiling at  $(220 \pm 15)$  °C was collected. Bromomethylacetate was purchased from TCI America. All the chemicals were of analytical grade and used as received.

**Nuclear Magnetic Resonance (NMR):** The molecular structure of NCT was determined by  $^1\text{H}$  and  $^{13}\text{C}$  NMR (Vega-300 Varian Inc, USA) and FT-IR (Nicolet 380 FT-IR) spectroscopic techniques. NMR experiments were done on a Vega-600 Varian spectrometer using the WATERGATE program (Varian Inc. USA).

**Rheology:** Dynamic rheological experiments were performed on an AR2000 stress controlled rheometer (TA Instruments). Samples were run at 25 °C using parallel plate geometry (20 mm diameter). Both frequency and stress sweeps were performed. Frequency sweeps were conducted in the linear viscoelastic regime of each sample, as determined previously by stress-sweep experiments (0 to 100% strain at 1 Hz). The gel was also subjected to a dynamic stress sweep, where the moduli were monitored as a function of the stress-amplitude at a constant frequency of 10 rad/s.

**Small Angle Neutron Scattering (SANS):** The experiments were done on the NG-7 (30 m) beam line at NIST in Gaithersburg, MD. Neutrons with a wavelength of 6 Å were selected. Three sample-detector distances were used to obtain data over a range of wave vectors from 0.004 to 0.4 Å<sup>-1</sup>. Samples were studied in 2 mm quartz cells at 25 °C. Scattering spectra were corrected and placed on an absolute scale using NIST calibration standards. The data are shown as plots of the absolute intensity  $I$  versus the wave vector  $q = 4\pi\sin(\theta/2)/\lambda$ , where  $\lambda$  is the wavelength of incident neutrons and  $\theta$  the scattering angle.

**Microscopy:** AFM analysis was carried out on Bruker MultiMode 8 AFM. SEM analysis by Supra 55 VP scanning electron microscope on carbon substrates. TEM analysis was carried out on ZEISS 902 transmission electron microscope on carbon coated copper grids.

**Textural Profile Analysis:** To determine the textural/mechanical properties (hardness, cohesiveness, adhesiveness) of the gels, textural profile analysis (TPA) was performed using texture analyzer (TA.HDPlus, Stable Microsystems, UK). TPA involves applying large forces, which causes permanent structural deformation of the material. For TPA, uniaxial compression test, the sample was compressed uniaxially using a cylindrical probe (P/5, stainless steel, diameter: 5 mm) in two consecutive cycles. The cross-head was attached with 5 kg load cell and the probe moved at a test speed of 1 mm/sec to a distance of 5 mm in button mode. The obtained data was analyzed using “Exponent Lite” software provided along with the instrument. The peak force of (peak height after) the first compression cycle represents the hardness or firmness of the gel. Cohesiveness and adhesiveness of the gel were determined as the ratio of the positive work done during the 2nd cycle to that done during the 1st cycle and the negative work done during the 1st cycle, respectively.

## 2. Computational Details

**Dissipative Particle Dynamics (DPD) Simulations:** In the present work, structural properties, interfacial density, worm like micelle structure formation, potential energy and their dependence on the respective chemical species concentration and the solvent ratio were investigated in detail by DPD simulation. More specifically, such DPD investigation studied here could shed light on the interfacial behavior in toluene and its influence on the worm like micellization (WLM). The simulation box having dimensions of 36 x 18 x 18 (in DPD units), with periodic boundary conditions in all directions are used and simulated in the NVT canonical ensemble (particle number  $N$ , volume  $V$ , and temperature  $T$ ) using the DPD module of Accelrys Materials Studio<sup>®</sup> 5.0. In this simulation, all the units are measured in DPD units unless otherwise specified. Present simulation used the bead spring constant as 4 units and the average bond length is the equilibrium bond length between 0.7 and 0.8, having three DPD units of amplitude noise parameter, which satisfies the fluctuation-dissipation theorem, thus the system reached to an equilibrium temperature. A modified velocity-Verlet algorithm is used to integrate the fluid-particle motion in the system, which is dictated by Newton's 2<sup>nd</sup> law of motion. Two of the most important properties in DPD must be liquid compressibility and mutual solubility, which determines the properties of the surfactant like materials. For the present application, we used the simplest model consisting of NCT molecules represented by a simple harmonic spring in toluene solvent. The interaction parameters among the head, tail of NCT and toluene are computed via the Blend program in MS studio package. We used MS studio DPD module using velocity -Verlet algorithm, using a velocity correction factor (0.70) with a time step of 2.5 nanoseconds.

**DPD Model and Bead Selection Details:** The mesoscopic course-grain (CG) model (NCTs+Toluene) for simulation under boundary condition was considered to comprise of three beads, where the hydrophilic ( $-\text{SO}_3\text{H}$  side) and hydrophobic (alkyl tail with phenyl ring) components of NCTs were the head (H) and the tail (T) beads, respectively, while toluene as the solvent was considered to represent a single bead. The volume of the hydrophobic tail or hydrophilic head bead of NCT is approximately  $230 \text{ \AA}^3$ . The volume of one toluene bead (Tol) containing two toluene molecules is reported to be approximately  $184 \text{ \AA}^3$ . However, it is relatively smaller than the volume of the tail or head bead (Fig. S8). Therefore, based on the approximated size and the equal volume principle, the simulated NCT molecules, we selected each of them as  $T_1H_1$  to describe the mesoscopic structure the system where H as the hydrophilic head group and T -hydrophobic bead denotes the tail group of each of the NCT mixture. The course grain model colour codes are represented as follows:  $-\text{SO}_3\text{H}$  head bead (H): Green, Alkyl tail bead (T) of  $D_0$  : Pink,  $D_1$  : Blue,  $D_2$  : Sky blue and  $D_3$  : Magenta, where  $D_n$ 's represent the respective amphiphiles with 'n' accounting for different degrees of *cis*-unsaturation. The number of beads of the molecule in the present simulation is computed by dividing its molecular weight by the mass of the toluene molecule (**92.13842**).

COMPASS force field parameters were used in the Molecular mechanics of the software package during the optimization process of the system. The Flory-Huggins,  $\chi$  parameters, for these beads and the solvent were estimated using atomistic simulation that predicts the mesoscopic structure and particle-particle interaction parameters. All atomistic simulations were carried out in the Blend module of Materials Studio<sup>®</sup> on a PC at the ambient temperature using COMPASS force-field parameters. The simulation box included 150,000 DPD particles having 3 DPD unit of density. Using the theory of Groot and Rabone, the cut-off radius,  $r_c$ , computed was about 7.2 Angstroms, and simulated the system using the time step of 2.5

nanoseconds. The number of iterations for each simulation experiment was set at  $5 \times 10^4$  time steps, and the average deviation from incompressibility (dimensionless) was always less than  $3 \times 10^{-5}$ . Initially, the system was heated to approximately 338 K to equilibrate the liquid and cooled back to a temperature of 313 K for the production run where the results were recorded accordingly.] The Flory-Huggins interaction parameters,  $\chi_{ij}$  were translated into the DPD interaction parameters, which is calculated using Groot et. al's theory;  $a_{ij} = 25 + 3.57\chi_{ij}$ , for each  $i^{\text{th}}$  and  $j^{\text{th}}$  particle. The surfactant volume fraction,  $V_s$  was between 0.1 – 0.5 percentage, and the volume fractions of toluene and amphiphilic molecules are taken as  $V_T = (1 - V_s)/2$ .

**NAMD Molecular Dynamics and Density Functional Calculations:** NAMD molecular dynamics simulations were performed using CHARMM36 force field parameters and explicit solvent model using Carperinelo method 2000 version. Distances were maintained during molecular dynamics by freezing the  $C_1$  carbon atoms of each chain during and the calculations were carried out for 1.0 ns. The geometries of the highlighted pairs were then subject further optimization of their structure using first-principles density functional theory (DFT) calculations. During minimization, the inter- and intra-molecular energy was computed using the B3LYP exchange correlation functional with the 6-31G(d) basis set, as implemented in the GAMESS electronic structure code.

### 3. Rheology

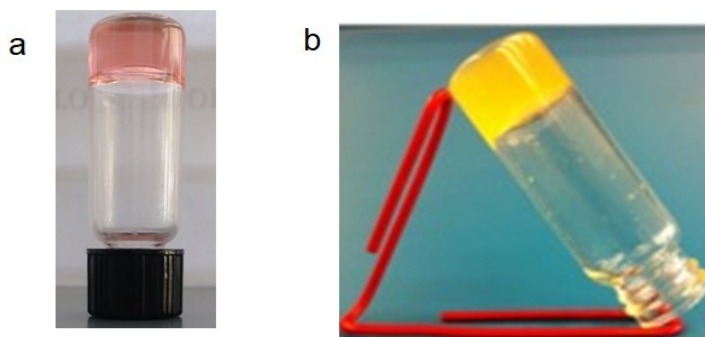


Fig. S1. Photographs of a) NCT with solubilized rhodamine6G in toluene b) NPPT in diesel

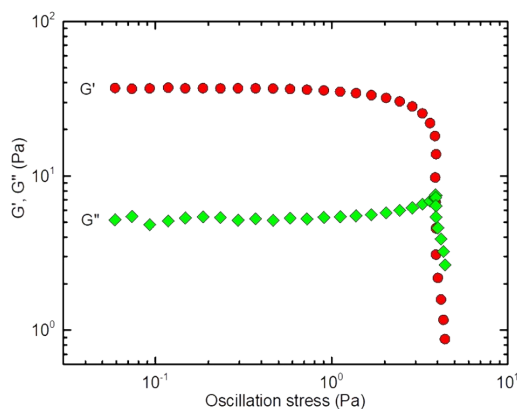


Fig. S2. Dynamic rheology of 2.0 wt% NPPT gel in toluene

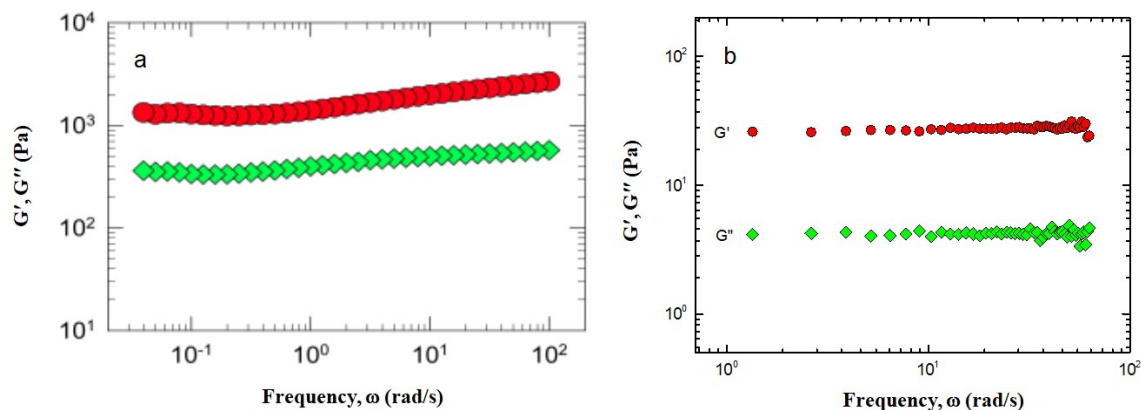


Fig. S3. Frequency sweep of 2.0 wt% of a) NCT gel in toluene and b) NPPT gel in toluene

#### 4. $^2\text{H}$ NMR studies

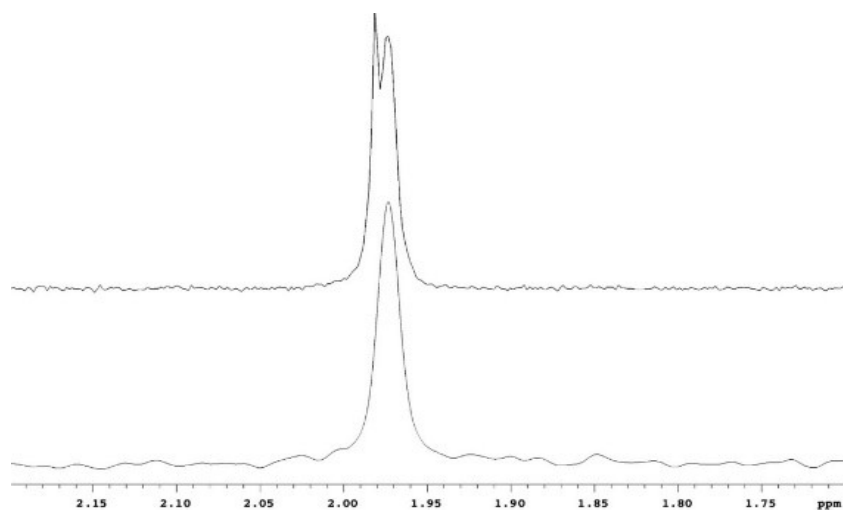


Fig. S4.  $^2\text{H}$  NMR of toluene gel of NCT grown in a capillary tube. TOP: showing two signals for the residual methyl protons of  $d_8$ -toluene. BOTTOM: neat  $d_8$ -toluene shown for comparison

In a typical experiment, an NCT gel (5 wt.%/v) in  $d_8$ -toluene was formed in a narrow capillary (2 mm diameter) and its  $^2\text{H}$  spectrum was recorded. The residual methyl protons of toluene at 2.8 ppm were split suggesting the presence of two magnetically nonequivalent  $-\text{CH}_3$  protons (of toluene) in the medium. (Fig.S4). A number of material phases such as bicelles,<sup>1</sup> liquid crystals<sup>2</sup> and polymers<sup>3</sup> in organic solvents demonstrate aligning ability when observed using residual dipolar coupling NMR. In the present case, the lengthier worm-like structures of NCT pervade in the gel structure resulting in the hydrophobic interlocks in the equilibrium gel state. The probability of interlocking increases, as the volume available for the growth of 1D reverse worms is highly restricted by the dimensions of the gelation tube. As a result, the worm-like structures experience a situation of maximum hydrophobic interlocks along the long axis of the tube. We speculate that the alignment tensors for the entrapped toluene molecules originate from the

strong steric effects provided by the hydrophobic pockets formed due to interlocks as well as from the competing  $\pi$ -stacking with the NCT molecules. Although, there is anisotropy between the two magnetically inequivalent protons, due to weak dipolar coupling, the alignment angle between the  $d_8$ -toluene and entrapped toluene is very less. Consequently, the splitting of signals becomes weak.

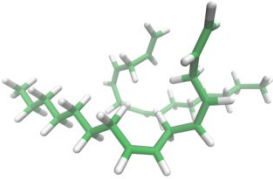
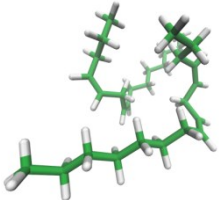
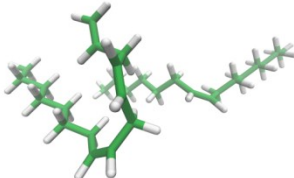
### 5. Gelation studies

**Table S1.** Gelation characteristics of NCT in various organic solvents (G- Gel; S- Soluble; P- Precipitate)

<b>SOLVENT</b>	<b>RESULT</b>	<b>MGC (wt%)</b>
Hexane	G	1.1
Diesel	G	1.5
Toluene	G	2.0
Water	S	-
2-Butanone	G	1.2
Cyclohexanol	G	1.5
Butanol	G	1.5
Methyl laurate	G	1.2
Heptanone	G	1.2
Cyclohexane	G	1.2
Xylene	G	1.2
Isooctane	P	-

## 6. Molecular Dynamics (MD) simulations

**Table S2.** Comparison of interaction energies and visually investigated amount of lipid chain “hooking” from molecular dynamics simulations for each pair of lipids

HOOKING COMBINATION	SNAPSHOT WITH ENERGY	INTERLIPID $sp^2$ DISTANCE <sup>[a]</sup>	BOND LENGTHS <sup>[b]</sup>
<b>C15_3 + C15_3</b>	 <p>B3LYP/N31: -0.00002469 eV</p>	<b>[L1C<sub>15</sub>-L2C<sub>15</sub>] = 4.665154 Å</b>	C15_3 0.000154 (C <sub>8</sub> -C <sub>9</sub> ) -0.000022 (C <sub>11</sub> -C <sub>12</sub> ) 0.000410 (C <sub>14</sub> -C <sub>15</sub> ) <i>C15_3 0.000051 (C<sub>8</sub>-C<sub>9</sub>)</i> <i>0.000651 (C<sub>11</sub>-C<sub>12</sub>)</i> <i>0.000130 (C<sub>14</sub>-C<sub>15</sub>)</i>
<b>C15_2 + C15_2</b>	 <p>B3LYP/N31: -0.0525 eV</p>	<b>C15_2 + C15_2</b> [L1_C <sub>8</sub> -L2C <sub>9</sub> ] = 5.765706	C15_2 0.000491 (C <sub>8</sub> -C <sub>9</sub> ) 0.001919 (C <sub>11</sub> -C <sub>12</sub> )  <i>C15_2 0.000063 (C<sub>8</sub>-C<sub>9</sub>)</i> <i>0.000914 (C<sub>11</sub>-C<sub>12</sub>)</i>
<b>C15_1 + C15_3</b>	 <p>B3LYP/N31: -0.0696 eV</p>	<b>C15_1 + C15_3</b> [L1C <sub>9</sub> -L2C <sub>11</sub> ] = 5.608288	C15_1 0.001519 (C <sub>8</sub> -C <sub>9</sub> )  <i>C15_3 0.000381 (C<sub>8</sub>-C<sub>9</sub>)</i>
<p>[a] The inter-lipid <math>sp^2</math> distance, e.g., L1C<sub>x</sub>-L2C<sub>y</sub> corresponds to the optimized distance between the unsaturated carbon atoms, C<sub>x</sub> and C<sub>y</sub> of the two chains, L1 and L2, respectively and [b] Change in the unsaturated <math>sp^2</math> hybridized double bond lengths before (normal) and after (italic) the calculations.</p>			



## 7. Textural profile analysis

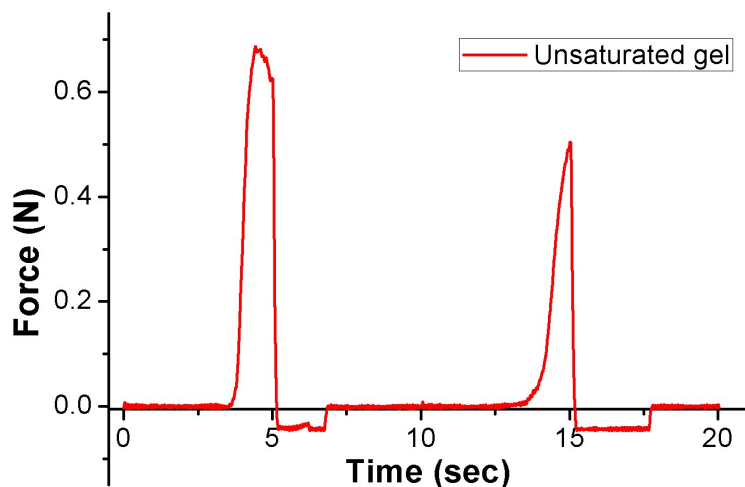


Fig. S5. Two-cycle uniaxial compression test of the NCT gel

**Table S3.** Textural parameters of the molecular gels and biopolymeric gels

Type of formulation	Hardness	Cohesiveness (%)	Adhesiveness (N.s)	References
NCTgel, 2 wt%	0.69 N	49	-0.07	--
NPPT gel, 2wt %	--	--		--
Gelatin, 10 wt%	40.08 N		-0.35	4
AMCS*, 10 wt%	1.10 N		-2.08	
Konjac gel <sup>#</sup>	2.38 N	90		5
Na-Alg*, 3 wt%	1.99 N	--	--	6
HPMC*, 3 wt%	3.37N	--	--	

## 8. Results and Discussion (DPD Simulation)

The self-assembly of the dynamics behavior of the micelle formation is studied with various simulation steps for NCT system in toluene solution. The mesoscale dynamic simulation is carried out with NCT concentrations from 2-3.3%. Therefore, in the simulation we used the ratio of NCT beads to toluene beads as ~2-3.37:97. The respective mesoscopic appearance of the system is shown in Fig. S8. Initially NCT beads were randomly distributed in toluene solution. With the increase in dynamic time-step, the NCT beads initiate to aggregate into small clusters and subsequently to small worm like micelles (WLMs). As the system approaches the equilibrium state (after 40,000 step), the NCT beads form more smaller WLMs and then long worm micelles, as shown in Fig. S8, and the morphology remains intact.

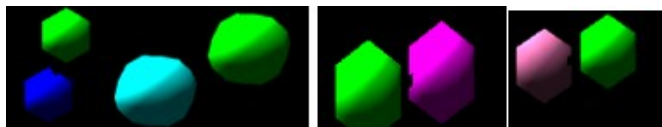


Fig. S6. *Bead description: Tail beads of D0 (Pink), D1 (Blue), D2 (Sky Blue) and D3 (Magenta), Hydrophilic head beads H in Green*

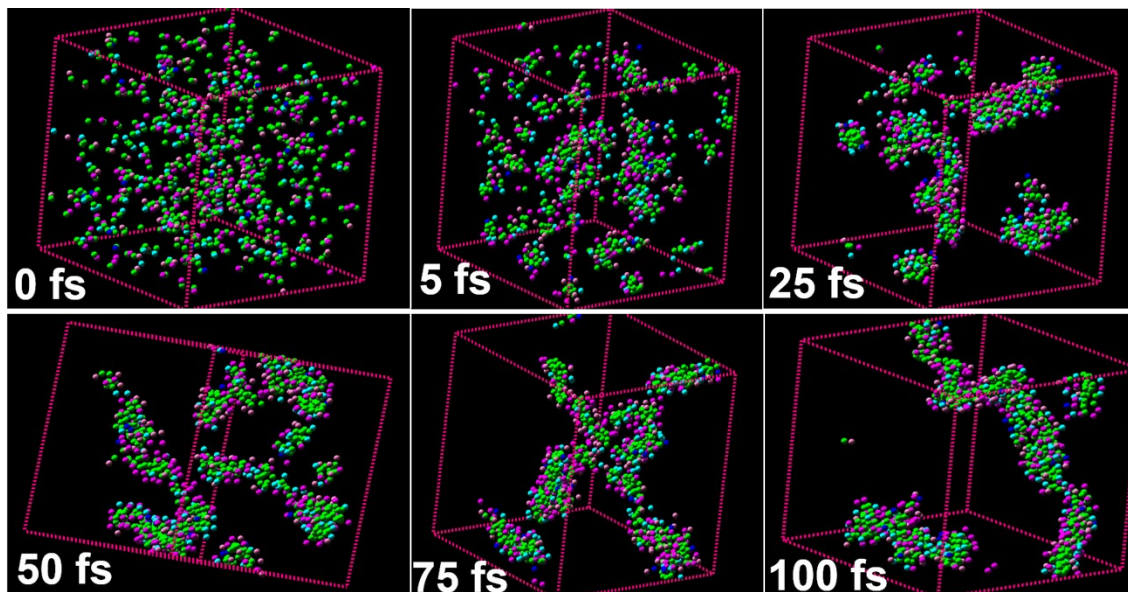


Fig. S7. *Snapshots collected from DPD simulation after different timescales depicting the growth of shorter and longer worm like micelles (periodic boundary conditions 20 X 20 X 20, NCT 2% and Toluene 98%)*

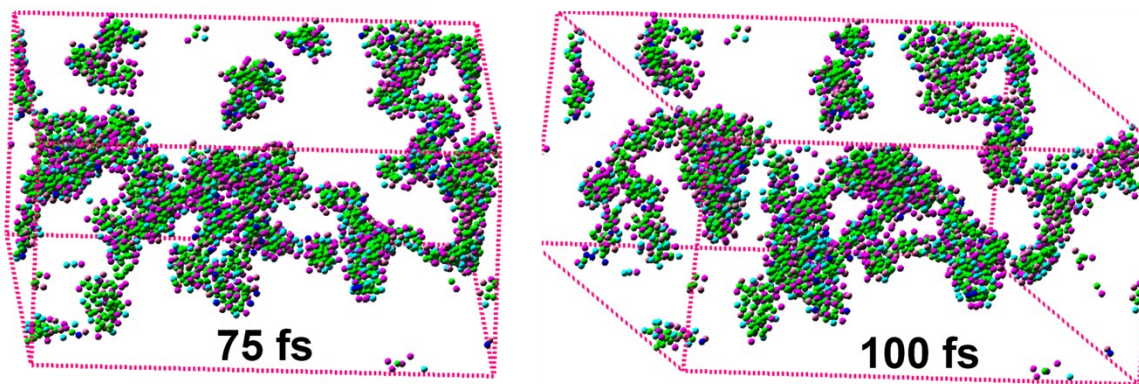


Fig. S8. *Snapshots collected from DPD simulation after different timescales depicting the growth of worm like micelles under periodic boundary conditions 40 X 40 X 20 (NCT 2% and Toluene 98%)*

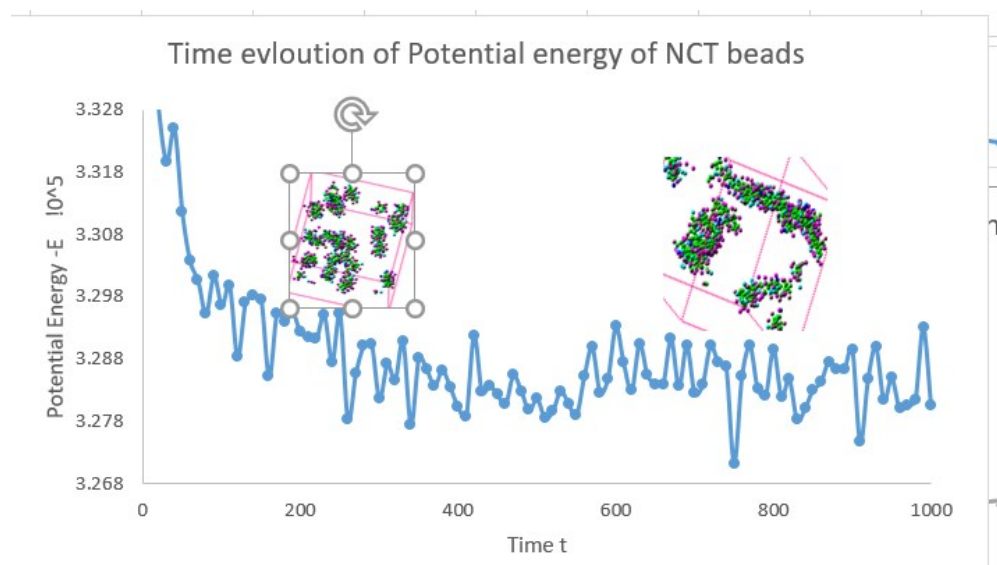


Fig. S9. Time evolution of Potential Energy of toluene-NCT (98:2) system under periodic boundary conditions 20X20X20

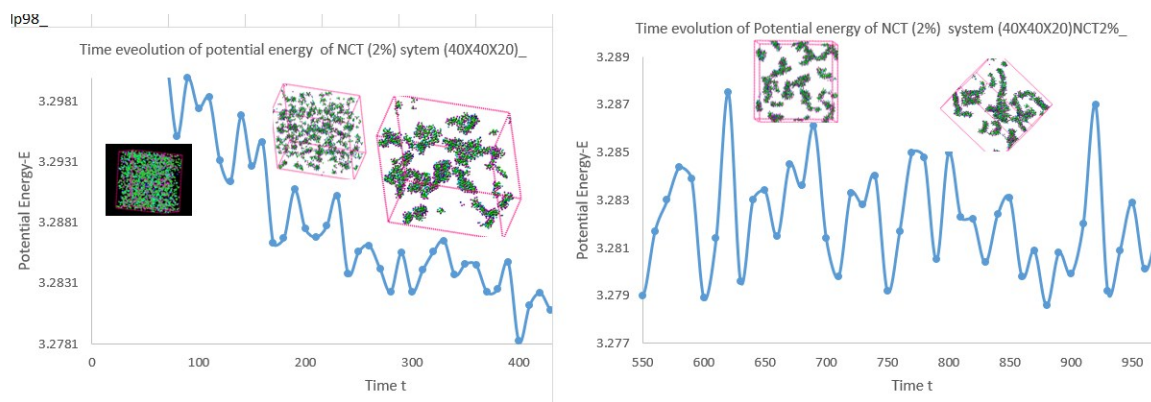


Fig. S10. Time evolution of Potential Energy of toluene-NCT (98:2) system under periodic boundary conditions 40 X 40 X 20 (left: 0 to 400 time-steps and right: 550 to 1000 time-steps).

This dynamic assembly process can also be monitored from the change in potential energy of the system with respect to the time-steps, as shown in Fig. S10.

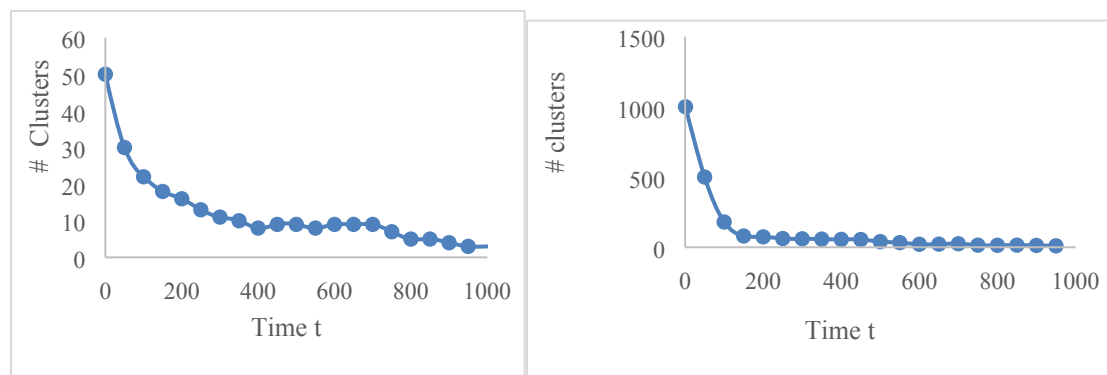


Fig. S11. Time evolution of number of clusters under boundary conditions  $20 \times 20 \times 20$  (left) and  $40 \times 40 \times 20$  (right)

Fig. S11 shows the total potential energy,  $E$  and the number of clusters that is formed during the simulation time. The total potential energy decreases rapidly with the decrease in the number of clusters or growth of clusters. However, once the clusters turn into worm-like micelles (WLMs), the change in potential energy becomes almost constant. This indicates that the potential energy is insensitive during the coalescence of smaller cluster into large WLMs formation. The largest approximate size of WLM is in between 14 to 40 Å within or under the dimension of  $40 \times 40 \times 20$  boundary condition.

**Effect of concentration:** As the concentration of the toluene decreased to 96.7%, we observed longer worm like structures due to higher concentration of NCT, as shown in Fig. S12.

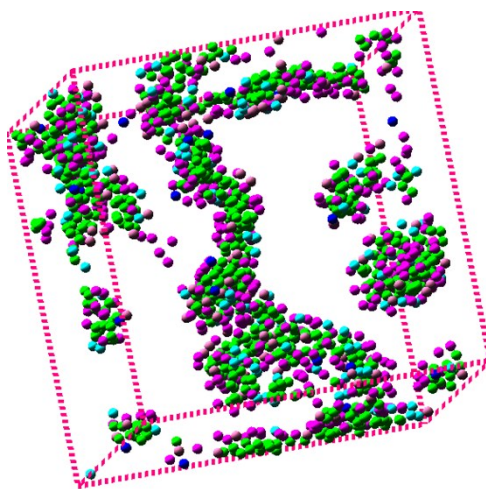


Fig. S12. Snapshots of the dynamic simulation at 350 time-step in toluene (96.7%) –NCT (3.3%) system. Toluene beads are excluded for clarity

At  $t = 350$  time step, the longest worm having an approximate contour length is  $\sim 38\text{-}43$  Å, as seen from Fig. S12. The respective kinetic energy for this system is shown below in Fig. S13.

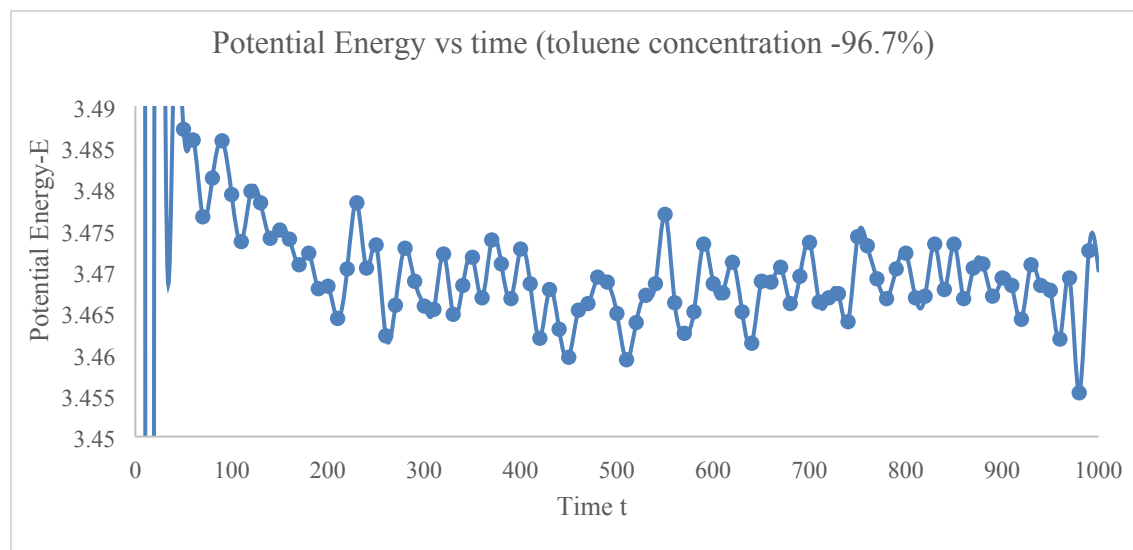


Fig. S13. Time evolution of potential energy for toluene (96.7%) –NCT (3.3%) system (periodic boundary conditions 20 X 20 X 20)

## 9. References

1. J. H. Prestegard, *Nat. Struct. Biol.* **1998**, *5*, 517- 522.
2. M. Rueckert, G. Otting, *J. Am. Chem. Soc.*, **2000**, *122*, 7793-7797.
3. J. C. Freudenberger, S. Knoer, K. Kobzar, D. Heckmann, T. Paululat, H. Kessler, B. Luy, *Angew. Chem. Int. Ed.* **2005**, *44*, 423 426.
4. P. H. M. Marfil, A. C. B. M. Anhô, V. R. N. Telis, *Food Biophysics* **2012**, *7*, 236.
5. F. Jiménez-Colmenero, S. Cofrades, A. M. Herrero, F. Fernández-Martín, L. Rodríguez-Salas, C. Ruiz-Capillas, *Food Hydrocolloids* **2012**, *26*, 63.
6. K. Rehman, M. C. I. Mohd Amin, M. H. Zulfakar, *Journal of Oleo Science* **2014**, *63*, 961.
7. V. V. Ginzburg, K. Chang, P. K. Jog, A. B. Argenton, L. Rakesh, *J. Phys. Chem. B*, **2011**, *115*, 4654-4661.
8. S. Plimpton, *J. Comp. Phys.*, **1995**, *11*, 1.